ChemComm

Palladium-Catalyzed Oxidative Homocoupling of Pyrazole Boronic Esters to Access Versatile Bipyrazoles and the Flexible Metal–Organic Framework Co(4,4′-bipyrazolate)

Journal:	*ChemComm*
Manuscript ID	CC-COM-11-2019-008614.R1
Article Type:	Communication

COMMUNICATION

Palladium-Catalyzed Oxidative Homocoupling of Pyrazole Boronic Esters to Access Versatile Bipyrazoles and the Flexible Metal–Organic Framework Co(4,4′-bipyrazolate)

Received 4th November 2019,
Accepted XXth December 2019

DOI: 10.1039/x0xx00000x

Mercedes K. Taylor,[a,b,c] Martin Juhl,[d] Gul Barg Hadaf, [d] Dasol Hwang, [d] Ever Velasquez,[c,e] Julia Oktawiec,[b] Jonathan B. Lefton,[f] Tomče Runčevski, [f] Jeffrey R. Long,[b,c,e]* Ji-Woong Lee[d]*

A facile route to 4,4′-bipyrazole (H_2bpz) and other symmetric bipyrazoles is acheived *via* the palladium-catalyzed homocoupling of a pyrazole boronic ester in the presence of air and water, enabling us to provide the first crystal structures and evidence of structural phase changes in the bipyrazolate-based metal–organic framework Co(bpz).

Pyrazole is a weakly-basic heterocyclic compound, and the deprotonated pyrazolate features two chemically-identical adjacent nitrogen atoms that comprise the basis for many transition-metal ligands.[1] The synthesis of substituted pyrazoles is an active area of research,[2] and these derivatives are of great interest in the pharmaceutical and agricultural industries due to their unique pharmacological effects.[3] Recently, pyrazoles and pyrazolates have also been incorporated into catalysts, energetic materials,[4] and sensing/electroluminescent materials.[5] The four coordinating nitrogen atoms of bipyrazolate anions can function as multitopic ligands, and these ligands have been shown to form extended coordination solids with various metals, yielding three-dimensional frameworks with diverse topologies.[6] The synthesis of bipyrazolate-based metal–organic frameworks has additionally led to significant advances in the properties of these adsorbents, including structural flexibility and gas storage capacities.[7] However, the simplest bipyrazolate ligand, 4,4′-bipyrazolate (bpz^{2-}), is underrepresented in this growing body of literature, owing to the synthetic difficulty of accessing 4,4′-bipyrazole (H_2bpz) and its functionalized derivatives.

Current syntheses of H_2bpz, as shown in Scheme 1, require multistep sequences (>9 steps)[8] or the use of volatile, hazardous reagents.[6a,9] Considering the symmetry and simplicity of the molecule, a desirable alternative route would be to synthesize H_2bpz through a pyrazole homocoupling reaction. It is commonly observed that symmetric biaryls are formed via the homocoupling of aryl halides (reductive, Ullmann-type)[10] or of aryl boronic acids (oxidative),[11] but this reactivity remains elusive in symmetric and dimeric heterocycles. Indeed, attempts to synthesize H_2bpz by coupling 4-iodopyrazole with itself in an Ullmann-type reaction have been unsuccessful.[6a] The Suzuki-Miyaura cross-coupling reaction offers a viable way to form a pyrazole–pyrazole bond,[12] but this reaction lacks the elegance and ease of homocoupling, as it requires both halopyrazole and pyrazole boronic acid starting materials. The absence of an efficient synthesis of bipyrazoles and their derivatives prompted us to develop a catalytic, scalable protocol to access these molecules, which would also promote the development of bipyrazolate-based metal–organic frameworks for various gas adsorption applications.

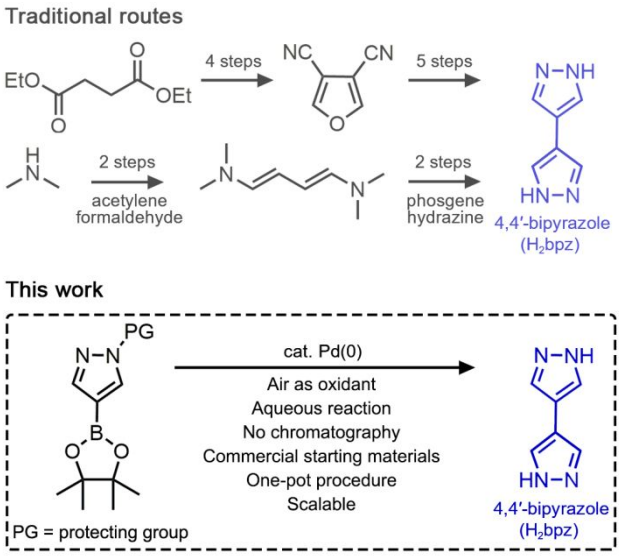

Scheme 1. Traditional routes to access 4,4′-bipyrazole (H_2bpz),[6a,8,9] and the catalytic homocoupling of pyrazoleboronic ester reported herein.

[a] *Center for Integrated Nanotechnologies, Sandia National Laboratories, Albuquerque, New Mexico 87185, USA*
[b] *Department of Chemistry, University of California, Berkeley, California 94720, USA*
[c] *Materials Sciences Division, Lawrence Berkeley National Laboratory, Berkeley, California 94720, USA*
[d] *Department of Chemistry & Nano-Science Center, University of Copenhagen, Copenhagen 2100, Denmark*
[e] *Department of Chemical and Biomolecular Engineering, University of California, Berkeley, California 94720, USA*
[f] *Department of Chemistry, Southern Methodist University, Texas 75205, USA*
Electronic Supplementary Information (ESI) available at DOI: 10.1039/x0xx00000x

We began our investigation with the commercially-available 1-methyl-4-pyrazoleboronic acid pinacol ester (**1a**) as a model substrate. The methyl moiety serves as a protecting group to prevent coordination to the palladium catalyst and was chosen over other common protecting groups both to facilitate monitoring of product formation via the methyl ^{1}H NMR signal and to improve solubility, as H_2bpz is not soluble in most common organic solvents. Demethylation conditions for pyrazole have been well established,[13] allowing for a straightforward deprotection after coupling.

To develop an efficient, selective reaction for the homocoupling of **1a**, we performed intensive screening to optimize the oxidant, base, solvent, and catalyst, among other variables (Table S1). Under optimized reaction conditions, high isolated product yields (up to 70%) were obtained with catalytic amounts (5 mol %) of $Pd(PPh_3)_4$ in the presence of 1 equiv of Cs_2CO_3 (Scheme 2, top). With these optimized reaction conditions, we evaluated the versatility and scalability of our protocol at the 1-gram scale using compound **1b**, a commercially-available 4-pyrazoleboronic acid pinacol ester featuring a tetrahydropyran (THP) protecting group (Scheme 2, bottom). Gratifyingly, the desired product (**2b**) was precipitated from aqueous solution in 81% yield after removal of the THP groups using a mild, one-pot deprotection procedure. The advantages of this methodology are numerous. The one-pot procedure is performed under air using an aqueous reaction mixture, and a straightforward work-up affords the desired product in high purity without the need for additional chromatography or recrystallization steps. A number of other symmetric bipyrazoles could also be generated under our reaction conditions (Scheme S1), highlighting the applicability of this route to many other molecules of interest for the development of coordination chemistry broadly and metal–organic frameworks in particular.

Pure H_2bpz (**2b**) obtained via this route was then found to react with a cobalt(II) source under solvothermal conditions to yield the metal–organic framework Co(bpz)[6b] as a microcrystalline, purple solid (see ESI for synthetic details). The material was purified by washing with *N,N′*-dimethylformamide (7 days) followed by dichloromethane (3 days) and was then activated by heating at 160 °C under dynamic vacuum for 16 h. The pure material was characterized by elemental analysis, infrared spectroscopy, powder X-ray diffraction, and scanning electron microscopy (see ESI). Synchrotron powder X-ray diffraction data obtained for the desolvated material revealed the crystal structure of Co(bpz) for the first time (Figure 1). The framework features one-dimensional rhombohedral channels that run along the crystallographic *c* axis and are lined with bpz^{2-} ligands and chains of cobalt(II) ions. A Langmuir surface area of 1060 m^2/g was determined from the 77-K N_2 adsorption data, consistent with the literature value[6b] and indicative of a highly porous material.

Notably, we also observed a distinct step in the isotherm at low N_2 pressures (~0.02 mbar; Figure 2, top, blue), a phenomenon not previously reported for this framework. This feature was reproducible across isotherms collected for several different Co(bpz) samples, and it is an indication of a structural phase change in which the framework undergoes a discrete expansion to a higher porosity structure at a given N_2 pressure. Interestingly, a step was also observed in the CO_2 adsorption isotherm at 195 K (~25 mbar; Figure 2, top, green), while H_2 adsorption in this material at 77 K adopts a Type 1 isotherm shape (Figure 2, bottom).

To determine the origin of the unusual gas adsorption isotherm features, we collected *in situ* synchrotron X-ray powder diffraction data for an activated sample of Co(bpz) gradually cooled from 298 to 165 K in the presence of 70 mbar CO_2 (Figure 3, top). Each diffraction pattern was indexed to obtain unit cell parameters for Co(bpz) as the decreasing temperature caused increasing amounts of CO_2 to adsorb onto the framework, and the obtained unit cell volumes are structurally revealing (Figure 3, bottom). From 298 to 207 K, the unit cell gradually contracts as the diamond-shaped channels become narrower, likely to better interact with adsorbed CO_2 molecules inside the channels. At 207 K, the abrupt appearance of new diffraction peaks corresponds to an abrupt increase in unit cell volume, indicating that Co(bpz) has undergone a discrete phase change to a structurally expanded structure, as is discussed further in the ESI. This unit cell data mirrors the CO_2 adsorption isotherm, in which initial CO_2 adsorption is followed by a sharp increase in gas uptake that indicates a discrete phase change. Thus, the X-ray powder diffraction data indicates that the steps apparent in the gas adsorption data are due to structural flexibility in Co(bpz).

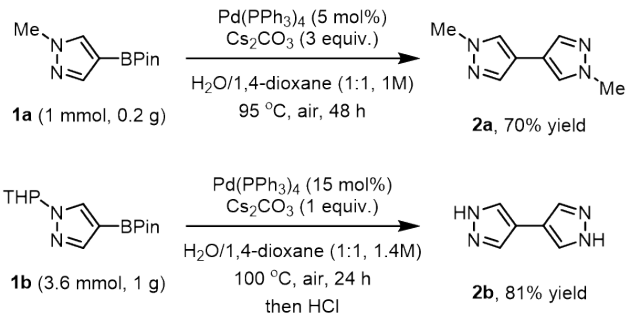

Scheme 2. Optimized conditions for the palladium-catalyzed oxidative homocoupling of **1a** (top) and **2a** (bottom).

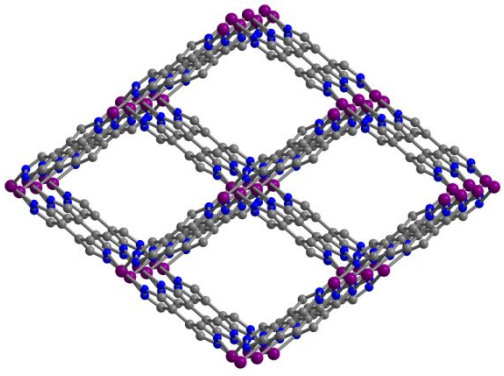

Figure 1. Powder X-ray diffraction structure of activated Co(bpz) at 298 K. Gray, blue, and purple spheres represent C, N, and Co atoms, respectively. H atoms have been omitted for clarity.

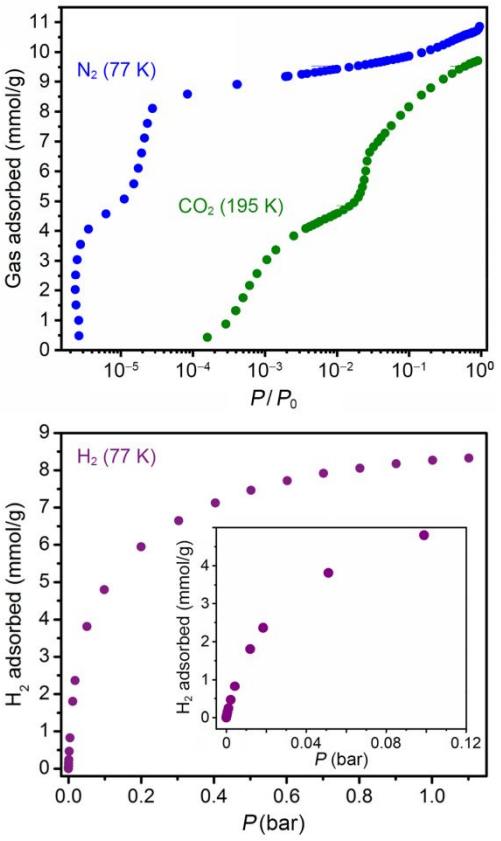

Figure 2. (Top) Gas adsorption isotherms for N_2 (77 K, blue) and CO_2 (195 K, green) in Co(bpz). The steps indicate structural flexibility, a property previously unobserved in this framework. (Bottom) H_2 adsorption isotherm for Co(bpz) at 77 K with the low-pressure region expanded in the inset. No H_2-induced phase changes were observed for Co(bpz) at this temperature.

In addition to this guest-induced flexibility, diffraction data collected under vacuum at 298 and 433 K revealed that Co(bpz) exhibits a reversible temperature-induced structural change. These two data sets could be solved to obtain two distinct crystal structures, shown in Figure 4, representing an increase in symmetry from *C*2/*c* to *Ccc*2 upon heating. In the 298 K structure, a distortion of the bpz^{2-} ligands breaks their internal planarity and allows each H atom to point towards the center of a neighboring aromatic ring, an energetically stabilizing interaction. Upon heating to 433 K, however, the bpz^{2-} ligands become fully planar, as is evident in the crystal structure when viewed down the *c* axis, and this change is accompanied by an expansion of the unit cell (Figure 4, bottom). Such reversible temperature-induced phase changes are not commonly observed in metal–organic frameworks and are of significant fundamental interest.[14] Our discovery of adsorption- and temperature-induced phase changes in Co(bpz) highlights the importance of a facile H_2bpz synthesis, since other bipyrazolate-based metal–organic frameworks are likely to possess similar flexibility and merit further in-depth study.

As shown in Figure 2, the phase-change behavior of Co(bpz) is guest-dependent: while adsorption of CO_2 and N2 results in a transition from a partially-expanded to a more fully-expanded phase, no phase change is observed upon adsorption of H_2 at the temperatures and pressures measured. The absence of a step in the H_2 isotherm may indicate that framework-H_2 interactions at 77 K are not strong enough to stabilize the partially-expanded phase, a hypothesis consistent with the relatively low binding strength of H_2 compared to other adsorbates. Furthermore, the partially-expanded phase achieved in the presence of N_2 or CO_2 occurs at a loading of 1 mol gas/mol Co(bpz) (see Figure S11). Given that the phase change is associated with one-to-one adsorption of guest molecules and is stabilized by N_2 and CO_2 but not H_2, the behavior is likely driven by the energetics of specific adsorbate-framework interactions, in addition to the energetics of the various framework conformations. This adsorbate-specific structural response is a desirable materials property that can potentially be leveraged for gas sensing or separation applications. Indeed, there is an ongoing effort to discover new flexible frameworks that meet industrial criteria for gas adsorption applications, as materials such as the flexible metal¬organic framework Co(bdp) (bdp^{2-} = 1,4-benzene-dipyrazolate) have shown significant promise for CH_4 storage and CO_2/CH_4 separation due to advantages associated with

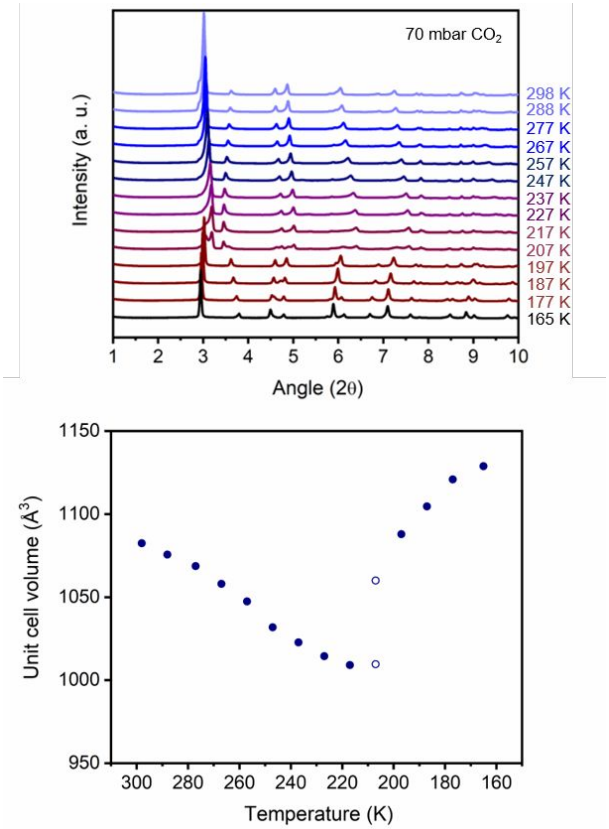

Figure 3. (Top) Powder X-ray diffraction data for Co(bpz) dosed with 70 mbar CO_2 over a range of temperatures. Changes in peak positions indicate structural phase changes induced by CO_2 adsorption. Colors are for clarity only. All data were collected at λ = 0.45241 Å. (Bottom) Unit cell volume of Co(bpz) dosed with 70 mbar CO_2 as the temperature decreases from left to right (obtained from the diffraction data above). The 207 K data set could not be fit to a single set of unit cell parameters but instead fit well to two distinct sets of unit cell parameters, represented by open circles (see ESI).

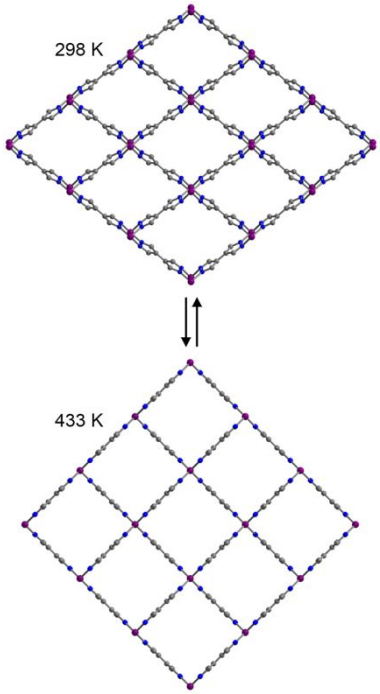

Figure 4. Powder X-ray diffraction structures of evacuated Co(bpz) at 298 K (top) and 433 K (bottom). Gray, blue, and purple spheres represent C, N, and Co atoms, respectively. H atoms have been omitted for clarity.

their structural flexibility.[7d,7g,17] Because Co(bpz) possesses the notable advantage of long-term stability to air and moisture (Figure S28), in contrast to its expanded analogue Co(bdp), our discovery of reversible structural flexibility in Co(bpz) is a significant advance in the development of flexible metal–organic frameworks and brings chemists closer to achieving synthetic control over all the properties necessary for a given industrial separation.

Ultimately, the synthesis of H_2bpz reported here greatly reduces the number of steps and hazardous reagents used in preparation of this valuable ligand, compared with previous methods, as well as eliminates the need for air-free techniques and column chromatography. This work renders Co(bpz) and other bipyrazolate frameworks increasingly accessible, opening the way to further advances in the synthesis of flexible metal–organic frameworks for gas adsorption applications.

Conflicts of interest

There are no conflicts to declare.

Notes and references

1 S. Trofimenko, *Chem Rev.*, 1972, **72**, 497.
2 (a) S. Onodera, T. Kochi, and F. Kakiuchi, *J. Org. Chem.*, 2019, **84**, 6508. (b) K. N. Tu, S. Kim, and S. A. Blum, *Org. Lett.*, 2019, **21**, 1283. (c) Y. Xu, X. Qi, P. Zheng, C. C. Berti, P. Liu, and G. Dong, *Nature*, 2019, **567**, 373. (d) F. Yi, W. Zhao, Z. Wang, and X. Bi, *Org. Lett.*, 2019, **21**, 3158.
3 (a) S. Fustero, M. Sánchez-Roselló, P. Barrio, and A. Simón-Fuentes, *Chem. Rev.*, 2011, **111**, 6984. (b) M. F. Khan, M. M. Alam, G. Verma, W. Akhtar, M. Akhter, and M. Shaquiquzzaman, *Eur. J. Med. Chem.*, 2016, **120**, 170. (c) A. Ansari, A. Ali, M. Asif, and Shamsuzzaman, *New J. Chem.*, 2017, **41**, 16.
4 C. Ye, G. L. Gard, R. W. Winter, R. G. Syvret, B. Twamley, and J. M. Shreeve, *Org. Lett.*, 2007, **9**, 3841.
5 (a) K. Dedeian, J. Shi, N. Shepherd, E. Forsythe, and D. C. Morton, *Inorg. Chem.*, 2005, **44**, 4445. (b) E. Cavero, S. Uriel, P. Romero, J. L. Serrano, and R. Giménez, *J. Am. Chem. Soc.*, 2007, **129**, 11608. (c) I. V. Taydakov, A. A. Akkuzina, R. I. Avetisov, A. V. Khomyakov, R. R. Saifutyarov, and I. C. Avetissov, *J. Lumin.*, 2016, **177**, 31.
6 (a) I. Boldog, J. Sieler, A. N. Chernega, K. V. Domasevitch, *Inorg. Chim. Acta*, 2002, **338**, 69. (b) C. Pettinari, A. Tăbăcaru, I. Boldog, K. V. Domasevitch, S. Galli, and N. Masciocchi, *Inorg. Chem.*, 2012, **51**, 5235. (c) S. Spirkl, M. Grzywa, C. S. Zehe, J. Senker, S. Demeshko, F. Meyer, S. Riegg, and D. Volkmer, *Crystengcomm.*, 2015, **17**, 313. (d) S. Spirkl, M. Grzywa, S. Reschke, J. K. H. Fischer, P. Sippel, S. Demeshko, H.-A. Krug von Nidda, and D. Volkmer, *Inorg. Chem.*, 2017, **56**, 12337.
7 (a) H. J. Choi, M. Dincă, and J. R. Long, *J. Am. Chem. Soc.*, 2008, **130**, 7848. (b) V. Colombo, C. Montoro, A. Maspero, G. Palmisano, N. Masciocchi, S. Galli, E. Barea, and J. A. R. Navarro, *J. Am. Chem. Soc.*, 2012, **134**, 12830. (c) Z. R. Herm, B. M. Wiers, J. A. Mason, J. M. van Baten, M. R. Hudson, P. Zajdel, C. M. Brown, N. Masciocchi, R. Krishna, and J. R. Long, *Science*, 2013, **340**, 960. (d) J. A. Mason, J. Oktawiec, M. K. Taylor, M. R. Hudson, J. Rodriguez, J. E. Bachman, M. I. Gonzalez, A. Cervellino, A. Guagliardi, C. M. Brown, P. L. Llewellyn, N. Masciocchi, and J. R. Long, *Nature*, 2015, **527**, 357. (e) C. Pettinari, A. Tăbăcaru, and S. Galli, *Coord. Chem. Rev.*, 2016, **307**, 1. (f) M. K. Taylor, T. Runčevski, J. Oktawiec, M. I. Gonzalez, R. L. Siegelman, J. A. Mason, J. Ye, C. M. Brown, and J. R. Long, *J. Am. Chem. Soc.*, 2016, **138**, 15019. (g) M. K. Taylor, T. Runčevski, J. Oktawiec, J. E. Bachman, R. L. Siegelman, H. Jiang, J. A. Mason, J. D. Tarver, and J. R. Long, *J. Am. Chem. Soc.*, 2018, **140**, 10324.
8 (a) E. C. Kornfeld and R. G. Jones, *J. Org. Chem.*, 1954, **19**, 1671. (b) S. Trofimenko, *J. Org. Chem.*, 1964, **29**, 3046.
9 Z. Arnold, *Collect. Czech. Chem. C,* 1962, **27**, 2993.
10 J. Hassan, M. Sévignon, C. Gozzi, E. Schulz, and M. Lemaire, *Chem. Rev.*, 2002, **102**, 1359.
11 (a) C. Adamo, C. Amatore, I. Ciofini, A. Jutand, and H. Lakmini, *J. Am. Chem. Soc.*, 2006, **128**, 6829. (b) K. Lee, and P. H. Lee, *Tetrahedron Lett.*, 2008, **49**, 4302.
12 L. Jedinák, R. Zátopková, H. Zemánková, A. Šustková, and P. Cankař, *J. Org. Chem.* 2017, **82**, 157.
13 (a) D. E. Butler and H. A. DeWald, *J. Org. Chem.*, 1975, **40**, 1353. (b) B. Pelcman, A. Sanin, P. Nilsson, K. No, W. Schaal, S. Öhrman, C. Krog-Jensen, P. Forsell, A. Hallberg, M. Larhed, T. Boesen, H. Kromann, S. B. Vogensen, T. Groth, and H.-E. Claesson, *Bioorg. & Med. Chem. Lett.*, 2015, **25**, 3024.
14 (a) G. Kumari, K. Jayaramulu, T. K. Maji, and C. Narayana. *J. Phys. Chem. A* **2013**, *117*, 11006. (b) M. Mączka, T. A. Da Silva, W. Paragasu, M. Ptak, and K. Hermanowicz. *Inorg. Chem.* **2014**, *53*, 12650. (c) J. Wieme, K. Lejaeghere, G. Kresse, and V. Van Speybroeck, *Nat. Comm.* **2018**, *9*, 4899.
15 J.-R. Li, J. Sculley, and H.-C. Zhou, *Chem. Rev.*, 2012, **112**, 869.
16 F.-X. Coudert, M. Jeffroy, A. Fuchs, A. Boutin, and C. Mellot-Draznieks, *J. Am. Chem. Soc.*, 2008, **130**, 14294.
17 (a) R. Kitaura, K. Seki, G. Akiyama, and S. Kitagawa, *Angew. Chem., Int. Ed.*, 2003, **42**, 428. (b) X. Zhao, B. Xiao, A. J. Fletcher, K. M. Thomas, D. Bradshaw, and M. J. Rosseinsky, *Science*, 2004, **306**, 1012. (c) H. Noguchi, A. Kondoh, Y. Hattori, H. Kanoh, H. Kajiro, and K. Kaneko, *J. Phys. Chem. B*, 2005, **109**, 13851. (d) P. L. Llewellyn, P. Horcajada, G. Maurin, T. Devic, N. Rosenbach, S. Bourrelly, C. Serre, D. Vincent, S. Loera-Serna, Y. Filinchuk, and G. Feŕey, *J. Am. Chem. Soc.*, 2009, **131**, 13002. (e) C. M. McGuirk, T. Runčevski, J. Oktawiec, A. Turkiewicz, M. K. Taylor, and J. R. Long, *J. Am. Chem. Soc.*, 2018, **140**, 15924.

Table of Contents image (3.4 cm x 8 cm):

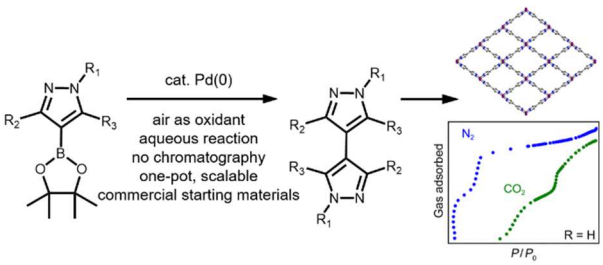

Table of Contents text:

A facile catalytic protocol achieves the homocoupling of pyrazole boronic esters, enabling access to the structurally-flexible metal–organic framework Co(bpz).